

## Article

# Chitosan/Selenium Nanoparticles Attenuate Diclofenac Sodium-Induced Testicular Toxicity in Male Rats

Samy M. El-Megharbel <sup>1,\*</sup>, Fawziah A. Al-Salmi <sup>2</sup>, Sarah Al-Harathi <sup>1</sup> , Khadeejah Alsolami <sup>3</sup>  
and Reham Z. Hamza <sup>2</sup>

<sup>1</sup> Chemistry Department, College of Sciences, Taif University, P.O. Box 11099, Taif 21944, Saudi Arabia; Sarah.alharathi@tu.edu.sa

<sup>2</sup> Biology Department, College of Sciences, Taif University, P.O. Box 11099, Taif 21944, Saudi Arabia; f.alsalmi@tu.edu.sa (F.A.A.-S.); Reham.z@tu.edu.sa (R.Z.H.)

<sup>3</sup> Pharmacology and Toxicology Department, College of Pharmacy, Taif University, P.O. Box 11099, Taif 21944, Saudi Arabia; K.alsolami@tu.edu.sa

\* Correspondence: s.megherbel@tu.edu.sa

**Abstract:** The detrimental effect of diclofenac sodium (Diclo-Na) on male reproductive organs is reported upon in this paper. Chitosan is a polysaccharide composed of various amounts of glucosamine. Chitosan nanoparticles (CH-NPs) have attracted much attention owing to their biomedical activity. Selenium (Se) has a vital role in nutrition, plays an important role in enhancing male reproduction, and has a wide range of free radical scavenging activities. However, the study of the impact of chitosan nanoparticles in combination with Se (IV) (CH-NPs/Se) on male reproductive toxicity associated with Diclo-Na administration is lacking in recent literature. The current study assessed the ameliorative effects of complexes of CH-NPs/Se (IV) on Diclo-Na and the ways in which they alter reproductive toxicity in male rats. Male rats were treated for 30 days successively, either with Diclo-Na (10 mg/kg) or co-treated with a CH-NPs/Se complex (280 mg/kg). Sperm characteristics, marker enzymes of testicular function, LH, FSH, and testosterone were evaluated in addition to oxidative stress markers and histological alterations. CH-NPs/Se significantly alleviated Diclo-Na-induced decline in sperm count and motility, testicular function enzymes, and levels of LH and testosterone in serum. Additionally, CH-NPs/Se co-administration at 280 mg/Kg, inhibited the Diclo-Na-induced decline of antioxidant enzyme activities and elevated oxidative stress indices and reactive free radicals in testicular homogenates of male rats. CH-NPs/Se (280 mg/kg) alone improved Diclo-Na and ameliorated histological damages in exposed rats. In conclusion, chitosan improved testicular function in Diclo-Na-treated rats by enhancing the testosterone hormone levels, ameliorating testicular tissue, and inhibiting markers of oxidative stress in male rats.

**Keywords:** male reproduction; selenium; diclofenac-sodium; oxidative stress markers; chitosan nanoparticles



**Citation:** El-Megharbel, S.M.; Al-Salmi, F.A.; Al-Harathi, S.; Alsolami, K.; Hamza, R.Z. Chitosan/Selenium Nanoparticles Attenuate Diclofenac Sodium-Induced Testicular Toxicity in Male Rats. *Crystals* **2021**, *11*, 1477. <https://doi.org/10.3390/cryst11121477>

Academic Editors: Assem Barakat and Alexander S. Novikov

Received: 26 October 2021

Accepted: 25 November 2021

Published: 28 November 2021

**Publisher's Note:** MDPI stays neutral with regard to jurisdictional claims in published maps and institutional affiliations.



**Copyright:** © 2021 by the authors. Licensee MDPI, Basel, Switzerland. This article is an open access article distributed under the terms and conditions of the Creative Commons Attribution (CC BY) license (<https://creativecommons.org/licenses/by/4.0/>).

## 1. Introduction

Diclofenac monosodium (Diclo-Na) is a non-steroidal anti-inflammatory drug (NSAID) that has high biological activity, is analgesic, and is a potential inhibitor of pain and rheumatic inflammation [1]. Diclofenac is used globally for the treatment of inflammation, pain, and degenerative joint diseases [2].

About 940 tons of Diclo-Na are consumed yearly [3]. Although Diclo-Na is an effective anti-inflammatory drug, it has many harmful side effects that are associated with the inhibition of prostaglandin biosynthesis. Diclo-Na is well documented to be related to the induction of oxidative injury [4].

Previous studies have documented that Diclo-Na treatment adversely affected the reproductive system [5]. The placental transfer of Diclo-Na has been reported previously [6]. Diclo-Na usage has been reported to cause marked reduction in testes weight and sperm

count, with the main degeneration taking place in the histological structure of the testes [7]. The metabolism of Diclo-Na has been associated with excessive ROS production, which induces oxidative stress and death by progressive apoptosis [8]. Hence, this study was conducted with the aim of minimizing the harmful effects of Diclo-Na on the male reproductive system.

Chitosan, an abundant natural polysaccharide, is the N-deacetylated product of chitin. Chitosan is well studied because of its numerous features, including biocompatibility, safety, and wide biodegradability [9]. Chitosan-based agents are active in diabetes prevention and treatment. Chitosan was also reported to possess strong antioxidant activity relative to pure selenite [10].

Chitosan is a polysaccharide compound composed of various amounts of glucosamine, linked by glycosidic bonds. It is a powder derived from several types of the compound chitin, which is widely found in the outer shells of crustacean species such as shrimps and crabs [10].

Chitosan nanoparticles (CH-NPs) have multiple ameliorative effects, such as immunomodulatory effects and anticancer activities. Moreover, nanoparticles possess a potent surface warp, which produces more decay pressure with an increment in solubility [10].

Additionally, the incorporation of active compounds that possess antioxidant agents into nanoparticle coatings represents a novel step. CH-NPs have attracted high attention as biomedical active compounds, as they possess a broad spectrum of biological activities, such as immunostimulatory effects, anti-inflammatory activities, and free radicals (ROS) scavenging activities [11].

Selenium (Se) is a trace element essential for nutrition. Se forms are present in multi-dietary supplements [12]. Se is an essential element for the biosynthesis of several selenoproteins, such as glutathione peroxidase (GPx), which are mainly involved in prevention of oxidative stress and cellular death by apoptosis. Additionally, Se is essential for biosynthesis and sperm production and motility [13].

Deficiency in Se levels has been reported to be related to the fragility of sperm and a decline in the sperm characteristics. Recently, studies have shown that Se offers high protection against toxicity to testicular tissue sustained through food additives [14] and reproductive toxicity from cadmium exposure [15].

Nanoparticle formulations provide stable pharmaceutical bases for enhancing the bioavailability and therapeutic effectiveness of medication. CH-NPs have elevated immunity relative to large chitosan particles. Additionally, CH-NPs possess a stronger surface area; this produces increased solubility [16].

Several previous studies have shown that antioxidant administration can overcome the toxic effects of drugs; in particular, an antioxidant that can be utilized is chitosan.

Recently, there has been a shortage in data on the important role that chitosan may play in the alleviation of Diclo-Na-induced reproductive toxicity in male rats. Therefore, the current paper reports on the important role of CH-NPs/Se as a dietary supplement for toxicity alleviation.

## 2. Materials and Methods

### 2.1. Chemicals

Commercial chemicals were used without purification from Sigma-Aldrich. Chitosan with a low molecular weight (60–190 kDa) and 80–85% degree of deacetylation, and selenium tetrachloride, Se (IV) with a purity  $\geq 98\%$ . The percentage of carbon, hydrogen, and nitrogen was measured using Vario EL Fab. CHN. The morphological surface was estimated using a Quanta FEG 250 scanning (SEM) and transmission (TEM) electron microscopes with 20 kV accelerating voltage, and the shapes and sizes of these particles were visualized using JEOL JEM-1200 EX II and JEOL 100s microscopes, respectively. Thermogravimetric analysis of the complexes was performed from room temperature to 800 °C using a TGA/DTA-50H Shimadzu thermal analyzer. The following were purchased

from Sigma Chemical Co. (St. Louis, MI, USA): diclofenac sodium and ELISA kits used for the assessment of F.S.H, L.H., and testosterone. All chemicals used for this study were of high analytical grade.

## 2.2. Synthesis of Se/Chitosan

A solution of 1% acetic acid was used to dissolve chitosan, and the resulting solution was filtered to remove impurities; we then added 2 M sodium hydroxide to the chitosan solution and stirred for 2 h. Then, the solution was filtered and washed using distilled water and the pH value was adjusted to 7–8. Next, the solution was frozen for 72 h. By using thiourea, purified chitosan was used for the preparation of (CH-NPs/Se) [17,18]. A total of 3.0 mmol of the purified chitosan was added to 140 mL of distilled water. Then, a solution of  $\text{SeCl}_4$  (Se (IV), 0.804 mmol in 60 mL distilled water) was added dropwise to the chitosan and the solution was stirred for 40 min to achieve homogeneity. Then, thiourea solution (0.0901 mmol) in 100 mL distilled water was added dropwise and was cooled for 3 h. Ethanol ( $\text{C}_2\text{H}_5\text{OH}$ ) was added to wash the (CH-NPs/Se) sample before drying for 48 h at 75 °C.

## 2.3. Experimental Animal Care

Forty male Wistar rats (age: 6 weeks old, 160–180 g) used in this study were obtained from the faculty of veterinary medicine, Zagazig University, Egypt. Experimental rats were kept in plastic cages under standard conditions: temperature of  $25 \pm 4$  °C and a natural photoperiod (12 h light/12 h dark cycle). They were provided free access to drinking water and food. The experimental procedures were executed according to the Guide for the Care and Use of Laboratory Animals by the National Institute of Health (NIH). The experiment was carried out according to approval number 39-31-0034 of Taif University.

## 2.4. Experimental Design

Experimental rats were assigned randomly into four main groups (10 rats each), and 280 mg/kg chitosan nanoparticles (CH-NPs/Se) [10] was administered following 10 mg/kg diclofenac–sodium Diclo-Na [5] administration by oral gavage for 30 successive days. The stock solutions of Diclo-Na and CH-NPs/Se were prepared daily before administration to the experimental animals. Diclo-Na was administered first, followed by CH-NPs/Se within 30 min of Diclo-Na administration in the combination group. Group 1, the control group, received distilled  $\text{H}_2\text{O}$  only. Group 2 was administered Diclo-Na (10 mg/kg) only. Group 3 was administered CH-NPs/Se (280 mg/kg) only. Group 4 (Diclo-Na + CH-NPs/Se) was co-administered Diclo-Na (10 mg/kg) and (CH-NPs/Se) (280 mg/kg), as shown in the experimental protocol (Figure 1).

On the last day of the experiment, blood samples were withdrawn from the retro-orbital venous plexus under light ether anesthesia. Then, the serum was obtained. The two testes were removed gently, weighed, and processed for histopathological and further biochemical analysis.

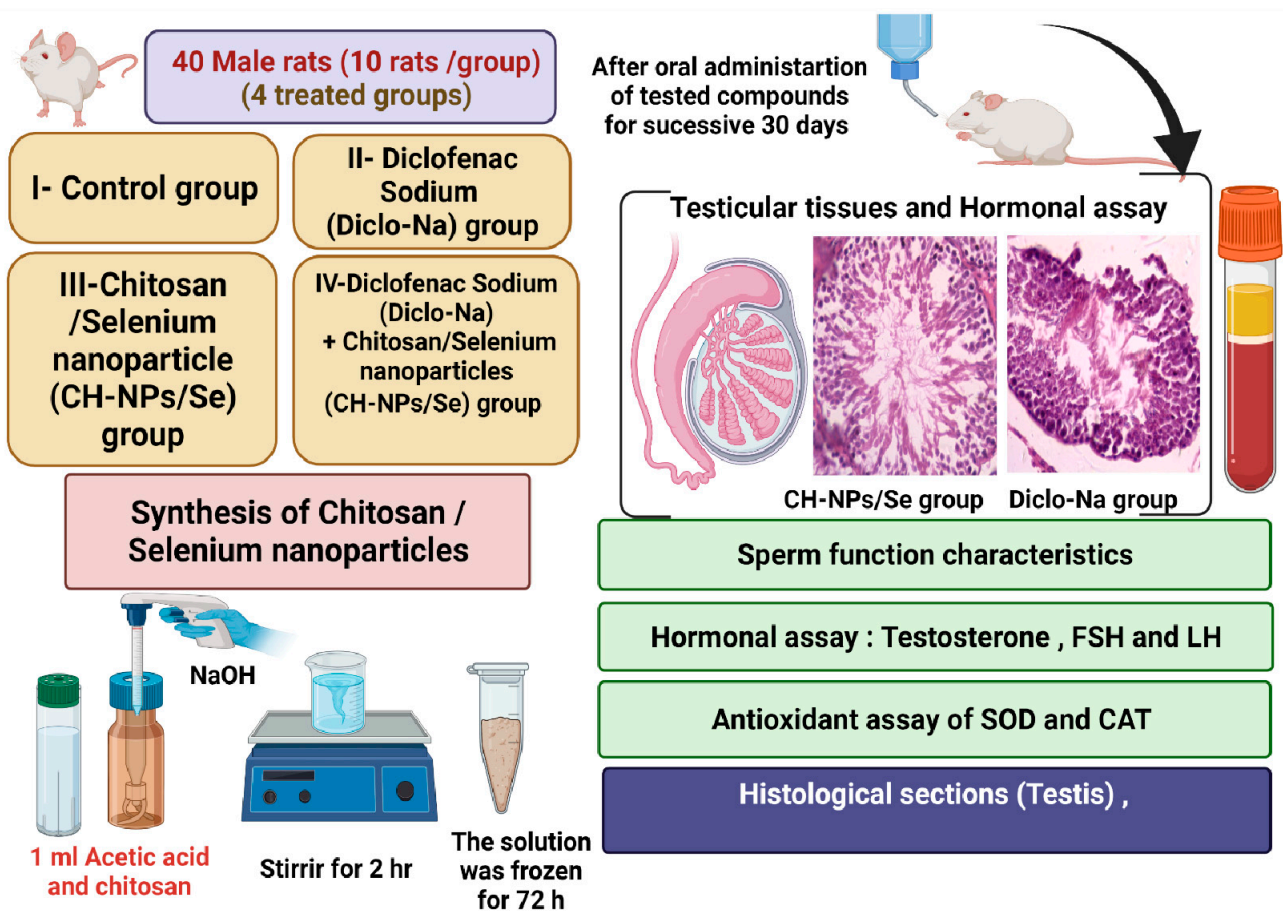


Figure 1. Experimental protocol.

### 2.5. Sperm Characteristics and Marker Enzymes of Testicular Function Assessment

Sperm abnormalities and viability were evaluated, and then epididymal spermatozoa were obtained and released onto the sterile glass slide. Approximately one drop of the diluted sperm suspension was mixed with freshly prepared stain and allowed to stand at 37 °C. We used a Neubauer chamber with the aid of a light microscope for scoring.

### 2.6. Assessment of Testosterone Hormone

Testosterone levels were estimated by ELISA kits. To reduce the inter-assay variation, all hormonal analyses were carried out simultaneously.

### 2.7. Assessment of Antioxidant and Oxidative Stress Indices

Small pieces of the testes were separated and homogenized using cold Tris-HCl buffer (pH 7.4) and were centrifuged to obtain the supernatant that was used for further biochemical assays. Superoxide dismutase (SOD) and catalase (CAT) activities were measured according to Beers and Sizer [19]. Glutathione peroxidase (GPx) activities were evaluated as described by Sedlak and Lindsay [20]. MDA (estimation of final marker of lipid peroxidation ROS) was measured as described earlier by Ohkawa et al. [21].

### 2.8. Histological Assessment

Microscopic assessment of the testes pieces was performed by using a standard method and staining with hematoxylin and eosin [22].

## 2.9. Statistical Analysis

Data were expressed as mean  $\pm$  SD. The values were analyzed using one-way ANOVA performed using GraphPad Prism (version 8.3.0). Values were considered statistically significant at  $p < 0.05$  [23].

## 3. Results

### 3.1. FTIR Studies

For the chitosan derivatives, the infrared spectral data (Figure 2) showed the main bands referring to functional groups. For chitosan, bands at  $3290\text{ cm}^{-1}$  represent the vibrational stretching motions of OH and  $\text{NH}_2$  groups. The bands at  $2920$  and  $2885\text{ cm}^{-1}$  represent the vibrational stretching motions of C–H, as explained in the literature [24]. The vibrational stretching at  $1635\text{ cm}^{-1}$  represent the amide I NH–CO group, whereas the NH–CO amide II group appears at  $1595\text{ cm}^{-1}$ , with vibrational bending motion due to the NH–CO amide group [25]. Bands in the ring structure of chitosan that appeared at  $1420$  and  $1335\text{ cm}^{-1}$  indicate the hydroxyl and carbon–hydrogen vibrations, respectively. The vibrational and bending motions for carbon–nitrogen of the NH–CO amide appeared at  $1278\text{ cm}^{-1}$ . The bands appeared between  $1150$  and  $800\text{ cm}^{-1}$  for chitosan, indicating the vibrational stretching of carbon–oxygen [25]. After chelation of chitosan selenium with chitosan, a shift appeared at  $3271\text{ cm}^{-1}$  for the stretching vibration of the amino group  $\text{NH}_2$ , and at  $2917\text{ cm}^{-1}$  for the C–H group; bands for the NH–CO amide group I and NH–CO amide group II appeared at  $1645$  and  $1555\text{ cm}^{-1}$ , respectively. Based on the above, the shifts in the band positions confirmed the chelation between selenium and chitosan [26,27].

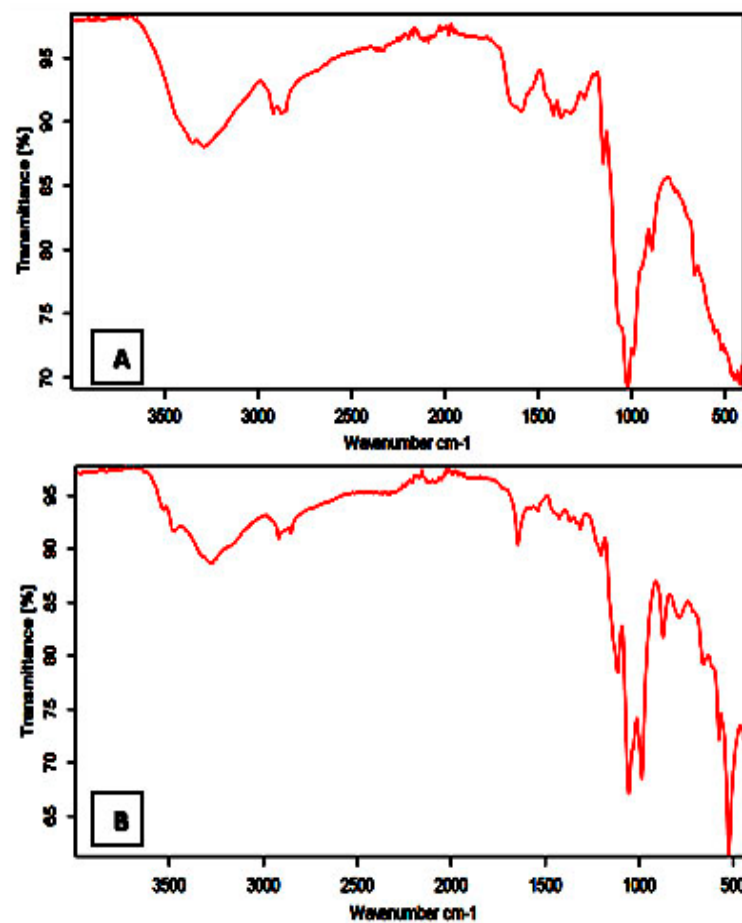


Figure 2. Infrared spectra of: (A) free ligand chitosan and its (B) Se/Chitosan complexity.

### 3.2. Thermal Analysis

For the CH-NPs complex, thermal degradation began at 50 °C, corresponding to a loss of moisture, which was in agreement with the literature [28]. For the chitosan complex, a degradation peak occurred between 270 and 380 °C, which was attributed to the loss of the CO<sub>2</sub> moiety [28]. There was a 5% temperature weight loss for Se/Chitosan, as shown in Table 1 [28]. The thermal behavior observed for the decomposition of Se/Chitosan confirmed the product's stability up to temperatures of 460 °C [28], and the final product of the thermal decomposition for the Se/Chitosan complex was SeO<sub>2</sub>.

**Table 1.** Thermal behavior of chitosan and its derivatives.

Sample Name	Weight Loss 5%	Weight Loss 10%	Weight Loss 20%	Residue %	Temperature of 1st Derivative Weight Loss
Chitosan	47.00 °C	71.98 °C	298.00 °C	21.08%	310.00 °C
Se/Chitosan	65.00 °C	93.00 °C	277.00 °C	25.95%	300.00 °C

### 3.3. XRD

For the (CH-NPs/Se) complex, XRD was carried out using an X-ray diffractometer with anodic copper, K-alpha [nm] = 0.154178, and the generator settings 3 of 0 mA, 40 KV. We used the Debye–Scherer equation,  $B = k\lambda/s \cdot \cos \theta$ , where  $s$  = crystallite size,  $\lambda$  = wavelength,  $k$  = constant taken as 0.94,  $\theta$  = diffraction angle (5.4947°), and  $B$  = full width at half maximum height (FWHM) (0.2509°). The crystallite size of the selenium (IV) complex was found to be 35 nm. Line broadening of the crystalline diffraction peak in the Se(IV) complex showed higher crystallinity of crystalline sizes associated with XRD data, ranging between 45 and 50 nm. The range of nanoparticle sizes was confirmed by the increasing molecular weight of the precursor; the increase for particle size  $r$  can be attributed to the larger atomic weights that enhance the merging of the crystal nucleus. This increases the density of nucleation centers in prepared complexes [29,30].

### 3.4. Scanning Electron Microscopy (SEM)

Scanning electron microscopy provides valuable information regarding the physical behavior of the selenium complex with chitosan nanoparticles (Figure 3). SEM cannot be used as a basic method to confirm the structure of the complex, but it can be used as a tool for identifying the presence of single components within a synthesized complex. The SEM for the selenium–chitosan complex showed a nano feature product with small-sized particles.

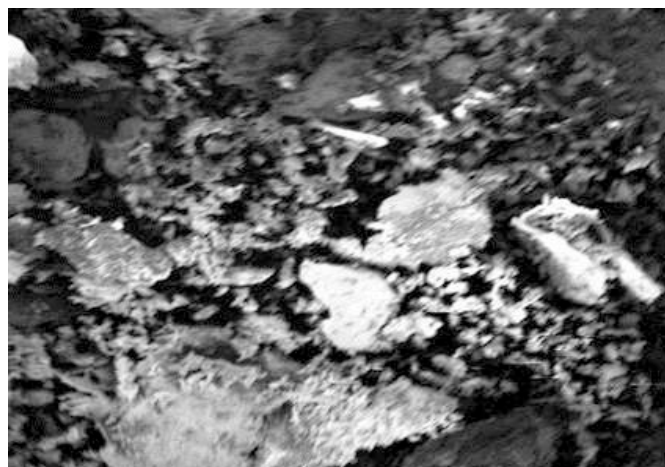


**Figure 3.** SEM image for CH-NPs/Se complexity.

### 3.5. Transmittance Electron Microscopy (TEM)

The TEM image for the CH-NPs/Se complex produced from reaction between Se (VI) and chitosan is displayed in Figure 4. After the chelation, the particle sizes were found to be in the range of 50 nm with black spherical spots, which was in agreement with the X-ray powder diffraction data.

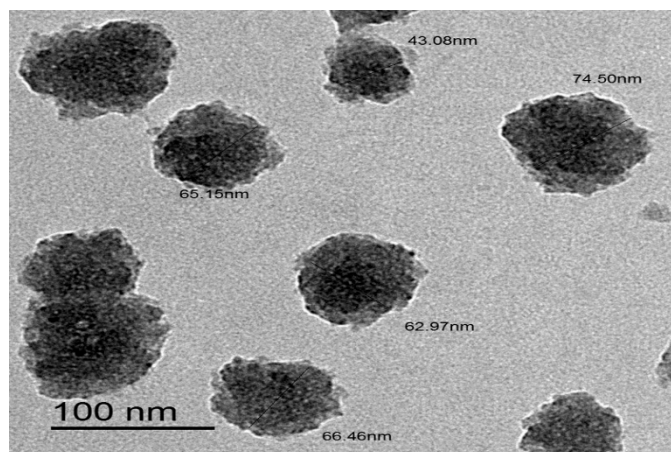


**Figure 4.** TEM of CH-NPs/Se complexes.

### 3.6. CH-NPs/Se Complex Improved Testosterone Hormone Levels and Sperm Characteristics in Diclo-Na Treated Rats

The novel CH-NPs/Se complex prevented the Diclo-Na-induced reduction in the level of testosterone hormone in male rats. The administration of Diclo-Na significantly decreased serum testosterone levels as compared with the control, although the novel CH-NPs/Se complex significantly ( $p < 0.05$ ) increased serum levels of testosterone compared to the Diclo-Na only group (Table 1). The novel CH-NPs/Se complex elevated ( $p < 0.05$ ) LH levels and maintained FSH levels as compared with Diclo-Na alone (Table 2). Meanwhile, sperm motility and viability were greatly improved in the group treated with a combination of the novel CH-NPs/Se complex and Diclo-Na, as shown in Table 3.

**Table 2.** Effect of CH-NPs/Se on serum reproductive hormones in male rats treated with Diclo-Na.

Title	Control	Diclo-Na	CH-NPs/Se	Diclo-Na + CH-NPs/Se
LH (ng/mL)	0.15 ± 0.01	0.10 ± 0.04 *	0.16 ± 0.03	0.13 ± 0.03 **
FSH (ng/mL)	0.80 ± 0.04	0.72 ± 0.01	0.82 ± 0.01	0.78 ± 0.01
Testosterone (ng/mL)	2.35 ± 0.02	1.02 ± 0.08 *	2.34 ± 0.01	2.06 ± 0.05 **

Values represent mean ± SD of 10 rats. \*  $p < 0.05$  versus control; \*\*  $p < 0.05$  versus Diclo-Na alone.

**Table 3.** Effect of CH-NPs/Se on sperm functional characteristics in male rats treated with Diclo-Na.

Title	Control	Diclo-Na	CH-NPs/Se	Diclo-Na + CH-NPs/Se
Count	98 ± 7.01	81.65 ± 6.05 *	99.28 ± 9.06	90.85 ± 5.33 **
Viability	96.11 ± 4.26	90.11 ± 5.43	96.90 ± 3.55	93.44 ± 4.23
Motility	91.00 ± 6.44	68.98 ± 4.28 *	91.15 ± 8.08	84.87 ± 5.13 **
Abnormality	4.68 ± 0.85	8.94 ± 1.06	4.79 ± 0.87	5.74 ± 0.88

Values represent mean ± SD of 10 rats. \*  $p < 0.05$  versus control; \*\*  $p < 0.05$  versus Diclo-Na alone.

### 3.7. CH-NPs/Se Complex Alleviated Diclo-Na-Induced Oxidative Stress in the Testicular Tissue

Diclo-Na administration reduced ( $p < 0.05$ ) antioxidant defense enzymes (CAT and SOD activities) in testicular tissue (Figure 5). CH-NPs reversed the Diclo-Na-mediated decrease in testicular function antioxidant markers.

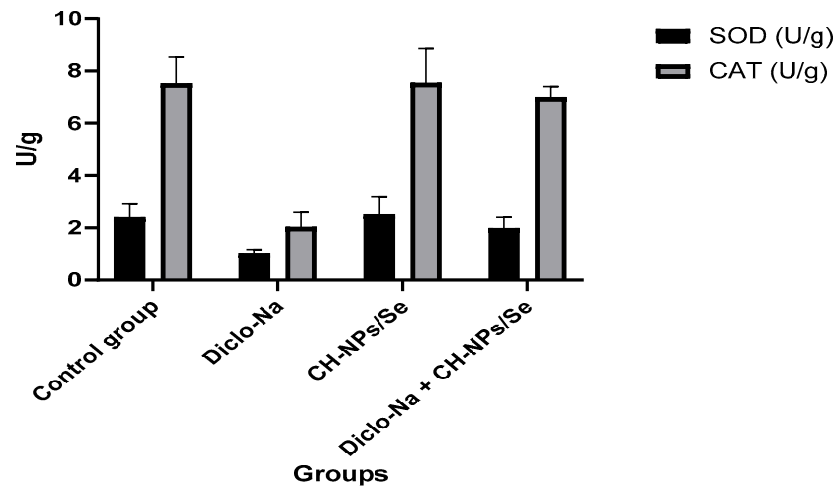


**Figure 5.** Effect of (CH-NPs/Se) on SOD and CAT activities in the testicular tissue of Diclo-Na-treated rats.

### 3.8. CH-NPs/Se Complex Improved Testicular Structure in Diclo-Na-Treated Rats

Diclo-Na induced a marked congestion in testicular tissue, whereas Diclo-Na and CH-NPs/Se co-treatment ameliorated the lesions induced by Diclo-Na in treated male rats. CH-NPs/Se evidently ameliorated Diclo-Na-induced testicular damage (Figure 6).

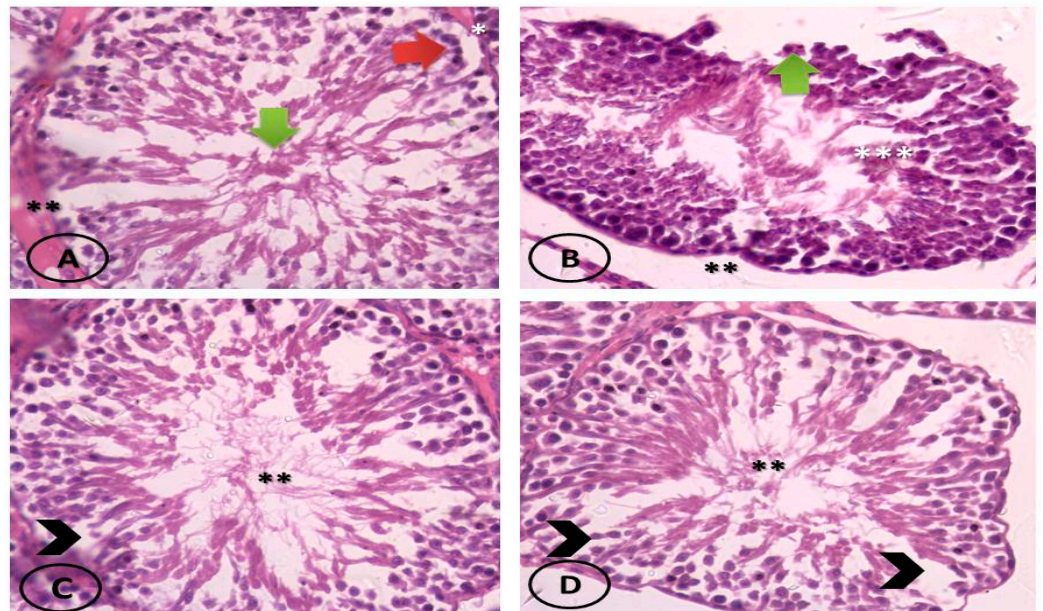


**Figure 6.** Photomicrograph of cross-section of (A) control group showing normal histological structure of seminiferous tubule and interstitial tissue (\*\*). The seminiferous tubules consists of normal somatic sperms (green arrow), and spermatogenic cells (red arrow), surrounded by peritubular myoid cells (\*). (H&E  $\times 400$ ). (B) Photomicrograph of cross-section of experimental mice after administration of toxic material. The seminiferous tubules contain some normal somatic sperms and showing toxicity in the form of degenerative changes of germ cells (\*\*\*), expansion of interstitial

space (\*\*), and disarrangement of spermatogonia with cellular debris (green arrow), with derangement of normal contours of the seminiferous tubules. (H&E  $\times 400$ ). (C) Photomicrograph of cross-section of chitosan/selenium-treated group showing normal histological structure of seminiferous tubules and interstitial tissue. The seminiferous tubules consist of normal somatic sperm (\*\*), and spermatogenic cells (arrowhead), surrounded by peritubular myoid cells, with a collection of Leydig cells in the intertubular area. (H&E  $\times 400$ ). (D) Photomicrograph of cross-section of experimental mice after administration of toxic material showing mild toxicity in the form of disarrangement and loss of some spermatogenic cells (arrowhead), presence of normal somatic sperm (\*\*), thinning and loss of interstitial tissue, and loss of peritubular myoid cells, resulting in expansion of the interstitial space. (H&E  $\times 400$ ).

#### 4. Discussion

Pharmaceuticals, including NSAIDs, are used widely as a treatment for health issues despite the many adverse effects associated with environmental contamination [31].

This study revealed that co-treatment with a novel complex (CH-NPs/Se) inhibited the reproductive toxicity associated with Diclo-Na in male rats. Hormonal control of testicular function acts through the endocrine pathway [32]. The basic endocrinal factors regulating the testicular functions are mainly testosterone, LH, and FSH in mammals [33].

Spermatogenesis is initiated when Leydig cells are activated by LH to produce the testosterone hormone, which conjugates with FSH [34] to enhance the spermatogenesis of Sertoli cells [35] and facilitates the germ cells' progression of spermatozoa and the nourishment of new sperm [36–39].

The decline in testosterone was accompanied by a clear decline in LH in Diclo-Na-treated rats; these are vital enzyme marker activities for spermatogenesis [5]. Meanwhile, an increment in testosterone hormone and antioxidant enzymes in rats treated with combination of CH-NPs/Se and Diclo-Na revealed the ameliorative effects of the novel complex (CH-NPs/Se) on Diclo-Na-induced reproductive toxicity. Therefore, CH-NPs/Se enhanced spermatogenesis and reduced Diclo-Na-induced testicular dysfunction.

The epididymis is responsible for the storage and maturation of the spermatozoa [40]. This study demonstrated that the novel complex (CH-NPs/Se) protects against Diclo-Na-induced reproductive toxicity and decline in the sperm characteristics.

Oxidative stress is often accompanied by the development of tissue injury. An oxidative burst involves a rapid increase in reactive oxygen species production, resulting in the oxidation of a diverse range of biological molecules, such as nucleic acids, lipids, and proteins [41]. The alleviation of this severe oxidative injury might be helpful for both ameliorating oxidation-induced testicular damage and controlling the activation of signaling cascades of protein kinases and cytokines [41].

From the point of view of histopathology, in the current study, the absence of essential spermatocytes indicated the impairment of spermatogenesis due to reduced testosterone levels induced by Diclo-Na. Moreover, the authors of [42] mentioned that treatment of male mice with Diclo-Na impaired seminiferous tubules and induced apoptosis in spermatogonia and spermatocytes as well as Sertoli and Leydig cells. These changes may lead to cellular toxicity accompanied by androgen disturbance [43,44].

These degenerative structural changes in the testes were not associated with any sort of lymphocyte aggregation and apoptosis that was induced by Diclo-Na. Interestingly, CH-NPs/Se nearly restored normal testicular structure.

Sertoli cells play a vital role in spermatogenesis [45]. Leydig cells are the main source of androgen production. These Sertoli cells can be affected by chemicals. Alteration in these cellular functions may lead to changes in the hormonal balance and may induce disturbance of male fertility [46].

Germ cells were degenerated in the Diclo-Na treated group [47]. Additionally, Diclo-Na had damaging effects on testicular structure [48].

The chitosan-containing selenium nano-formulation had a strong ameliorative effect on reproductive toxicity induced by Diclo-Na. The supplementation with different CH-NPs/Se lead to significant improvements in the reproductive tissues and hormonal level

in male rats. Chitosan/selenium nanoparticles (CH-NPs/Se) were significantly more effective than free Se-Na and CH-NPs, as reported previously by the authors of [49], in the prevention of oxidative stress and the improvement of antioxidant activity in testicular tissues of male rats. These chitosan/selenium nanoparticles can be encapsulated in a wide range of other dietary supplements to confer bioavailability to testicular tissues. Overall, these (CH-NPs/Se) have the potential to attenuate Diclo-Na reproductive toxicity and enhance antioxidant capacities.

## 5. Conclusions

In conclusion, we demonstrated that the novel CH-NPs/Se complexes had a potent effect against Diclo-Na-induced testicular toxicity and hormonal disturbance in male rats, in particular high oxidative stress, thus protecting against testicular necrosis and dysfunction. The enhancement of serum antioxidant enzymes by CH-NPs/Se indicated the possible antioxidant activity of this novel complex as an animal supplement. The antioxidant activity of CH-NPs/Se in the testicular tissues was also studied.

**Author Contributions:** Conceptualization, S.M.E.-M. and R.Z.H.; methodology, S.M.E.-M., F.A.A.-S. and R.Z.H.; validation, S.M.E.-M., S.A.-H., K.A. and R.Z.H.; formal analysis, S.M.E.-M., F.A.A.-S., K.A. and R.Z.H.; investigation, S.M.E.-M. and R.Z.H.; resources, S.M.E.-M., F.A.A.-S., K.A. and R.Z.H.; data curation, S.M.E.-M., S.A.-H., K.A. and R.Z.H.; writing—original draft preparation, S.M.E.-M., F.A.A.-S. and R.Z.H.; writing—review and editing, S.M.E.-M. and R.Z.H.; visualization, S.M.E.-M., F.A.A.-S., S.A.-H., K.A. and R.Z.H.; supervision, S.M.E.-M. and R.Z.H.; project administration, S.M.E.-M., S.A.-H. and R.Z.H.; funding acquisition, S.M.E.-M., S.A.-H., K.A. and R.Z.H. All authors have read and agreed to the published version of the manuscript.

**Funding:** This research received no external funding.

**Institutional Review Board Statement:** The study was conducted according to the guidelines of the Declaration of Helsinki and approved by the Ethics Committee of Taif University: 39-31-0034.

**Informed Consent Statement:** Not applicable.

**Data Availability Statement:** Data analyzed or generated during this study are included in this manuscript.

**Acknowledgments:** The authors acknowledge Taif University Researcher supporting project number (TURSP-2020/21), Taif University, Taif, Saudi Arabia.

**Conflicts of Interest:** The authors declare no conflict of interest.

## References

1. El-Megharbel, S.M.; Hamza, R.Z.; Refat, M.S. Synthesis, spectroscopic and thermal studies of Mg(II), Ca(II), Sr(II) and Ba(II) diclofenac sodium complexes as anti-inflammatory drug and their protective effects on renal functions impairment and oxidative stress. *Spectrochim. Acta Part A Mol. Biomol. Spectrosc.* **2015**, *135*, 915–928. [[CrossRef](#)]
2. Mousa, A.A.; Elweza, A.E.; Elbaz, H.T.; Tahoun, E.A.E.-A.; Shoghy, K.; Elsayed, I.; Hassan, E.B. Eucalyptus Globulus protects against diclofenac sodium induced hepatorenal and testicular toxicity in male rats. *J. Tradit. Complement. Med.* **2020**, *10*, 521–528. [[CrossRef](#)]
3. Zhang, Y.; Geißen, S.-U.; Gal, C. Carbamazepine and diclofenac: Removal in wastewater treatment plants and occurrence in water bodies. *Chemosphere* **2008**, *73*, 1151–1161. [[CrossRef](#)]
4. Ahmed, A.Y.; Gad, A.M.; El-Raouf, O.M.A. Curcumin ameliorates diclofenac sodium-induced nephrotoxicity in male albino rats. *J. Biochem. Mol. Toxicol.* **2017**, *31*, e21951. [[CrossRef](#)]
5. Owumi, S.E.; Aliyu-Banjo, N.O.; Odunola, O.A. Selenium attenuates diclofenac-induced testicular and epididymal toxicity in rats. *Andrologia* **2020**, *52*, e13669. [[CrossRef](#)]
6. Shintaku, K.; Hori, S.; Tsujimoto, M.; Nagata, H.; Satoh, S.; Tsukimori, K.; Nakano, H.; Fujii, T.; Taketani, Y.; Ohtani, H.; et al. Transplacental Pharmacokinetics of Diclofenac in Perfused Human Placenta. *Drug Metab. Dispos.* **2009**, *37*, 962–968. [[CrossRef](#)]
7. Vyas, A.; Purohit, A.; Ram, H. Assessment of dose-dependent reproductive toxicity of diclofenac sodium in male rats. *Drug Chem. Toxicol.* **2019**, *42*, 478–486. [[CrossRef](#)] [[PubMed](#)]
8. Inoue, A.; Muranaka, S.; Fujita, H.; Kanno, T.; Tamai, H.; Utsumi, K. Molecular mechanism of diclofenac-induced apoptosis of promyelocytic leukemia: Dependency on reactive oxygen species, akt, bid, cytochrome and caspase pathway. *Free. Radic. Biol. Med.* **2004**, *37*, 1290–1299. [[CrossRef](#)] [[PubMed](#)]

9. Abd-Elhakeem, M.A.; Mohamed, S.R.; Aya, H.R. Chitosan nanoparticles as hepato-protective agents against alcohol and fatty diet stress in rats. *J. Biochem. Int.* **2017**, *4*, 5–10.
10. Al-Baqami, N.; Hamza, R. Synergistic antioxidant capacities of vanillin and chitosan nanoparticles against reactive oxygen species, hepatotoxicity, and genotoxicity induced by aging in male Wistar rats. *Hum. Exp. Toxicol.* **2020**, *40*, 183–202. [[CrossRef](#)] [[PubMed](#)]
11. Hamza, R.; Al-Harbi, M.; Al-Hazaa, M. Neurological Alterations and Testicular Damages in Aging Induced by D-Galactose and Neuro and Testicular Protective Effects of Combinations of Chitosan Nanoparticles, Resveratrol and Quercetin in Male Mice. *Coatings* **2021**, *11*, 435. [[CrossRef](#)]
12. Abuelzahab, H.; Hamza, R.; Montaser, M.; El-Mahdi, M.M.; Al-Harhi, W.A. Antioxidant, antiapoptotic, antigenotoxic, and hepatic ameliorative effects of L-carnitine and selenium on cadmium-induced hepatotoxicity and alterations in liver cell structure in male mice. *Ecotoxicol. Environ. Saf.* **2019**, *173*, 419–428. [[CrossRef](#)]
13. Hamza, R.Z.; Al-Harbi, M.S.; El-Shenawy, N.S. Ameliorative effect of vitamin E and selenium against oxidative stress induced by sodium azide in liver, kidney, testis and heart of male mice. *Biomed. Pharmacother.* **2017**, *91*, 602–610. [[CrossRef](#)]
14. Hamza, R.Z.; Diab, A.E.-A.A. Testicular protective and antioxidant effects of selenium nanoparticles on Monosodium glutamate-induced testicular structure alterations in male mice. *Toxicol. Rep.* **2020**, *7*, 254–260. [[CrossRef](#)]
15. Alharhi, W.A.; Hamza, R.Z.; Elmahdi, M.M.; Abuelzahab, H.; Saleh, H. Selenium and L-Carnitine Ameliorate Reproductive Toxicity Induced by Cadmium in Male Mice. *Biol. Trace Element Res.* **2019**, *197*, 619–627. [[CrossRef](#)] [[PubMed](#)]
16. Hamza, R.Z.; El-Megharbel, S.M.; Altalhi, T.; Gobouri, A.A.; Alrogi, A.A. Hypolipidemic and hepatoprotective synergistic effects of selenium nanoparticles and vitamin. E against acrylamide-induced hepatic alterations in male albino mice. *Appl. Organomet. Chem.* **2020**, *34*, e5458. [[CrossRef](#)]
17. Dhillon, G.S.; Kaur, S.; Brar, S.K.; Verma, M. Green synthesis approach: Extraction of chitosan from fungus mycelia. *Crit. Rev. Biotechnol.* **2012**, *33*, 379–403. [[CrossRef](#)]
18. Fernández-Llamosas, H.; Castro, L.; Blázquez, M.L.; Díaz, E.; Carmona, M. Speeding up bioproduction of selenium nanoparticles by using *Vibrio natriegens* as microbial factory. *Sci. Rep.* **2017**, *7*, 16046. [[CrossRef](#)]
19. Beers, J.R.; Sizer, I.W. A Spectrophotometric Method for Measuring the Breakdown of Hydrogen Peroxide by Catalase. *J. Biol. Chem.* **1952**, *195*, 133. [[CrossRef](#)]
20. Sedlak, J.; Lindsay, R.H. Estimation of Total, Protein-Bound, and Nonprotein Sulfhydryl Groups in Tissue with Ellman's Reagent. *Anal. Biochem.* **1968**, *25*, 192. [[CrossRef](#)]
21. Ohkawa, H.; Ohishi, N.; Yagi, K. Assay for lipid peroxides in animal tissues by thiobarbituric acid reaction. *Anal. Biochem.* **1979**, *95*, 351. [[CrossRef](#)]
22. Hayat, M.A. (Ed.) *Basic Techniques for Transmission Electron Microscopy*, 1st ed.; Macmillan Press: New York, NY, USA, 1986; ISBN 9780123339263.
23. Dean, A.; Sullivan, K.; Soe, M. OpenEpi: Open Source Epidemiologic Statistics for Public Health. 2013. Available online: <https://www.OpenEpi.com> (accessed on 6 May 2013).
24. Bin, J.; Xiao, Y.; Lin, Z.; Deng, Y.L.; Chen, Y.; Le, D.E.; Bin, J.; Li, M.; Liao, Y.; Liu, Y.; et al. High molecular weight chitosan derivative polymeric micelles encapsulating superparamagnetic iron oxide for tumor-targeted magnetic resonance imaging. *Int. J. Nanomed.* **2015**, *10*, 1155–1172. [[CrossRef](#)]
25. Bujňáková, Z.; Dutková, E.; Zorkovská, A.; Baláž, M.; Kováč, J.; Kello, M.; Mojžiš, J.; Briančin, J.; Baláž, P. Mechanochemical synthesis and in vitro studies of chitosan-coated InAs/ZnS mixed nanocrystals. *J. Mater. Sci.* **2017**, *52*, 721–735. [[CrossRef](#)]
26. Liu, J.; Guo, T.-F.; Shi, Y.; Yang, Y. Solvation induced morphological effects on the polymer/metal contacts. *J. Appl. Phys.* **2001**, *89*, 3668–3673. [[CrossRef](#)]
27. Ryu, S.R.; Noda, I.; Jung, Y.M. What is the origin of positional fluctuation of spectral features: True frequency shift or relative intensity changes of two overlapped bands? *Appl. Spectrosc.* **2010**, *64*, 1017–1021. [[CrossRef](#)] [[PubMed](#)]
28. Mohammad, F.; Bwatanglang, I.B.; Yusof, N.A.; Abdullah, J.; Hussein, M.Z.; Alitheen, N.B.M.; Abu, N. Folic acid targeted Mn:ZnS quantum dots for theranostic applications of cancer cell imaging and therapy. *Int. J. Nanomed.* **2016**, *11*, 413–428. [[CrossRef](#)]
29. Lassoued, A.; Dkhil, B.; Gadri, A.; Ammar, S. Control of the shape and size of iron oxide ( $\alpha$ -Fe<sub>2</sub>O<sub>3</sub>) nanoparticles synthesized through the chemical precipitation method. *Results Phys.* **2017**, *7*, 3007–3015. [[CrossRef](#)]
30. Alagiri, M.; Hamid, S.B.A. Green synthesis of  $\alpha$ -Fe<sub>2</sub>O<sub>3</sub> nanoparticles for photocatalytic application. *J. Mater. Sci. Mater. Electron.* **2014**, *25*, 3572–3577. [[CrossRef](#)]
31. Christen, V.; Hickmann, S.; Rechenberg, B.; Fent, K. Highly active human pharmaceuticals in aquatic systems: A concept for their identification based on their mode of action. *Aquat. Toxicol.* **2010**, *96*, 167–181. [[CrossRef](#)]
32. Sofikitis, N.; Giotitsas, N.; Tsounapi, P.; Baltogiannis, D.; Giannakis, D.; Pardalidis, N. Hormonal regulation of spermatogenesis and spermiogenesis. *J. Steroid Biochem. Mol. Biol.* **2008**, *109*, 323–330. [[CrossRef](#)]
33. Ramaswamy, S.; Weinbauer, G.F. Endocrine control of spermatogenesis: Role of FSH and LH/testosterone. *Spermatogenesis* **2014**, *4*, e996025. [[CrossRef](#)] [[PubMed](#)]
34. O'Shaughnessy, P.J. Hormonal control of germ cell development and spermatogenesis. *Semin. Cell Dev. Biol.* **2014**, *29*, 55–65. [[CrossRef](#)] [[PubMed](#)]
35. Jones, R.E.; Lopez, K.H. *Chapter 4—Human Reproductive Biology*, 4th ed.; Elsevier Science Publishing Co. Inc.: San Diego, CA, USA, 2014.

36. Liang, J.; Wang, N.; He, J.; Du, J.; Guo, Y.; Li, L.; Wu, W.; Yao, C.; Li, Z.; Kee, K. Induction of Sertoli-like cells from human fibroblasts by NR5A1 and GATA4. *eLife* **2019**, *8*, e48767. [[CrossRef](#)]
37. Akhigbe, R.; Ajayi, A. Testicular toxicity following chronic codeine administration is via oxidative DNA damage and up-regulation of NO/TNF-alpha and caspase 3 activities. *PLoS ONE* **2020**, *15*, e0224052. [[CrossRef](#)]
38. Motawi, T.M.; Sadik, N.A.; Refaat, A. Cytoprotective effects of DL-alpha-lipoic acid or squalene on cyclophosphamide-induced oxidative injury: An experimental study on rat myocardium, testicles and urinary bladder. *Food Chem. Toxicol.* **2010**, *48*, 2326–2336. [[CrossRef](#)]
39. Aly, H.A.; Khafagy, R.M. Taurine reverses endosulfan-induced oxidative stress and apoptosis in adult rat testis. *Food Chem. Toxicol.* **2014**, *64*, 1–9. [[CrossRef](#)]
40. Adedara, I.A.; Abolaji, A.O.; Awogbindin, I.O.; Farombi, E.O. Suppression of the brain-pituitary-testicular axis function following acute arsenic and manganese co-exposure and withdrawal in rats. *J. Trace Elements Med. Biol.* **2017**, *39*, 21–29. [[CrossRef](#)]
41. AlBasher, G.; Abdel-Daim, M.M.; Almeer, R.; Ibrahim, K.; Hamza, R.Z.; Bungau, S.; Aleya, L. Synergistic antioxidant effects of resveratrol and curcumin against fipronil-triggered oxidative damage in male albino rats. *Environ. Sci. Pollut. Res.* **2019**, *27*, 6505–6514. [[CrossRef](#)]
42. AdeyemiJulius, W.J.; Omoniyi, J.A.; Olayiwola, A.; Ibrahim, M.; Ogunyemi, O.; Olayaki, L.A. Elevated reproductive toxicity effects of diclofenac after withdrawal: Investigation of the therapeutic role of melatonin. *Toxicol. Rep.* **2019**, *6*, 571–577.
43. Obeys, A.K.; Karim, A.; Mahood, S. Histological study of the effect of piroxicam on testes of albino mice *Mus musculus*. *J. Univ. Anbar. Pure Sci.* **2013**, *7*, 1–11.
44. Frungieri, M.B. Cyclooxygenase and prostaglandins in somatic cell populations of the testis. *Bioscientifica* **2015**, *149*, R169–R180. [[CrossRef](#)]
45. Saponi, P.M.H.; Chatelain, P.; Saez, J.M. In vitro interaction between Sertoli cells and steroidogenic cells. *Biochem. Biophys. Res. Commun.* **1986**, *134*, 957–962. [[CrossRef](#)]
46. Papadakis, V.; Vlachopapadopoulou, W.; Van Syckle, K. Gonadal function in young patients successfully treated for Hodgkin's disease. *Med. Pediatr. Oncol.* **1999**, *32*, 366–372. [[CrossRef](#)]
47. Campion, S. Male reprotoxicity and endocrine disruption. In *Molecular, Clinical and Environmental Toxicology. Experientia Supplementum*; Luch, A., Ed.; Springer International Publishing AG: Berlin, Germany, 2012; Volume 101, pp. 315–360.
48. Mohan, D.; Sharma, S. Histopathological alterations in liver of mice exposed to different doses of diclofenac sodium. *World Acad. Sci. Eng. Technol. Int. J. Anim. Vet. Sci.* **2017**, *11*, 698–702.
49. Araujo, J.M.; Fortes-Silva, R.; Pola, C.C.; Yamamoto, F.Y.; Gatlin III, D.M.; Gomes, C.L. Delivery of selenium using chitosan nanoparticles: Synthesis, characterization, and antioxidant and growth effects in Nile tilapia (*Oreochromis niloticus*). *PLoS ONE* **2021**, *16*, e0251786. [[CrossRef](#)]